Structural, Electrical and Dielectric Properties of Dodecylbenzene Sulphonic Acid Doped Polypyrrole/Nano-Y_2O_3 Composites

Muhammad Irfan[1] · Abdul Shakoor[1]

Abstract

We report a facile strategy to synthesized the PPy-DBSA-Y_2O_3 composites with increasing amount of Y_2O_3 (2%, 4% and 8%) by in situ polymerization method. The samples were characterized by XRD, FTIR, SEM and dielectric spectroscopy. Structural and morphological analysis reveals the conformation of composite formation, increase in crystallinity and particle size also increased by doping Y_2O_3 into PPy-DBSA matrix. The frequency dependent AC conductivity (σ_{ac}), dielectric constant (ε') and loss factor (ε'') were measured in the frequency range from 20 Hz to 1 MHz. All measured quantities; σ_{ac}, ε' and ε'' are enhanced with increase in Y_2O_3 content in the composites at all frequencies. Dielectric constant value for all samples is very high at low frequency however decreases with increase in frequency. Synthesis of PPy-DBSA-Y_2O_3 composite materials with a large dielectric constant is very important for the improvement of electronic devices applications.

Keywords AC conductivity · Dielectric constant · Dielectric loss · XRD · Nano-Y_2O_3

1 Introduction

Intrinsically conducting polymers (ICPs) have significant applications in electromagnetic shielding, electrical displays, rechargeable batteries, optical computers and molecular electronics, several types of sensors and actuators, smart structures in electronic devices, drug release systems, synthetic nerves and inducting exchange membranes [1–4]. One of the outstanding features of ICPs is that it is promising to control conductivity of these polymers over extensive range from insulating to metallic by proper doping, addition of fillers and by intercalating these polymers into different inorganic host materials such as TiO_2 [5], TaS_2 [6], $CdPS_3$ [7], V_2O_5 [8] and Y_2O_3 [9]. Intercalation of conducting polymers in the interlameller galleries of nano-Y_2O_3 clay has been explored by several researchers [10]. Clay based polymer composites have been focus of a large number of investigations during the past two decades because of their numerous engineering applications. These composites show better mechanical and thermal properties, cheap permeability for gases and flame retardant and fire dowsing characteristics

[4, 11, 12]. Intercalation of polymer into the clay galleries and exfoliation of nanostructured clay platelets in the polymer matrix provide exclusive combination of organic and inorganic components at molecular level which communicates synergistic properties to conducting polymer clay composites which cannot be achieved from individual components, such as enhanced and well-disciplined electrical conductivity [13], improved thermal stability and outstanding mechanical, barrier and anticorrosive properties [14, 15]. Composites of conducting polymers and nanostructured clays were used as conductive fillers in insulating polymer exhibits the increase in electrical conductivity and low percolation threshold [16] as compare with pure conducting polymer. Among several conducting polymers, polypyrrole (PPy) is one of the most studied conducting polymer, due to environmental stability, low cost, ease of synthesis and controlling their electrical properties [17]. PPy and its derivatives have been successfully employed in electronic devices as hole and electron transport semiconducting materials in transistors and LEDs [18, 19]. In the existing work, to understand the mechanism of conduction and dielectric properties may be valuable in developing the device performance and designing the electronic devices. The survey of literature reveals that the detailed conductivity/dielectric studies on PPy-DBSA-Y_2O_3 composites are scarce. Herein, we report the PPy-DBSA-Y_2O_3 composites prepared by in situ

✉ Muhammad Irfan
  mirfanphysics@gmail.com

1 Department of Physics, Bahauddin Zakariya University, Multan 60800, Pakistan

polymerization method and characterized these samples by XRD, FTIR, SEM and dielectric spectroscopy.

2 Experimental Details

The Pyrrole (Fluka) was refined under reduce pressure also stored at low temperature before to use. Ammonium persulphate (APS), dodecylbenzene sulfonic acid (DBSA) and yttrium oxide (Y_2O_3) were achieved from Sigma-Aldrich and used as obtained. The all materials were used as presented without any more purification.

2.1 Preparation of Polypyrrole (PPy)

The required amount of APS was isolated in 100 mL of de-ionized water and stirred for 1 h and then pyrrole was dissolved regularly within the suspension throughout the stirring at 5 °C. The monomer to oxidant molar ratio was kept 1:1. The suspension was left for 1 day for polymerization. Finally, the suspension was filtered and cleaned with de-ionized water until the filtrate turns to colorless. The greenish black paste of PPy was achieved which was desiccated at 60 °C in vacuum oven for 1 day.

2.2 Preparation of PPy-DBSA-Y_2O_3 Composite

The 0.15 mol of DBSA was dissolved in 100 mL of de-ionized water, 0.3 mol of Pyrrole was put in gradually in the mixture solution which was retained on magnetic stirring. 30% hydrochloric acid (HCl) was introduced into the reaction mixture to keep pH value 0 and 1 with strong magnetic stirring. To this solution, Y_2O_3 powder was dissolved into the polymerization mixture under stirring. After 1 h, the proper amount of APS was dissolved in 100 mL of de-ionized water drop wise under strong stirring for half hour period. The monomer/oxidant/dopant molar ratio was taken 1:1:1/4. Then, 1 L methanol was also incorporated into the mixture and kept it at room temperature for 2 days to attain complete polymerization. After all, the suspension was filtered and cleaned with de-ionized water up to filtrate changes to colorless. The greenish black paste of PPy-DBSA-Y_2O_3 was conquered which was desiccated at 60 °C in vacuum oven for 1 day.

2.3 Measurements

X-ray powder diffraction analysis was carried out employing automated diffractometer, Panalytical X'Pert PRO equipped with CuKα radiations ($\lambda = 1.54$ Å). The Fourier transform infrared spectra was recorded on KBr pellet samples in the range of 4000–500 cm^{-1} by using a Perkin-Elmer Fourier transforms infra-red spectrometer. Scanning electron

microscopy was carried out on an EVO50 ZEISS instrument. Dielectric and Conductivity were measured of pressed pellets by applying 10 ton pressure in stainless steel die of 4-mm in diameter and 1-mm thickness in press machine by using a two point technique in the frequency range 20 Hz to 1 MHz. The samples were connected to a Keithley 2400 electrometers and a current source electrometer.

3 Results and Discussion

3.1 Structural Analysis

The X-ray diffraction pattern for polypyrrole (PPy), PPy-DBSA and their composite of PPy-DBSA-Y_2O_3 are revealed in Fig. 1. Figure 1d shows the main crystalline peaks of Y_2O_3 nanoparticles observed at $2\theta = 29.46°$, 34.12°, 48.73° and 57.90° corresponds to periodicity d = 0.16, 0.14, 0.10 and 0.91 nm in the direction of (222), (400), (440) and (622) planes is in good agreement with that on the JCPD card S25-1200, which describes that the sample has cubic crystal system taking space group I213. Adopting Scherer's formula [20, 21], the calculated crystalline size of Y_2O_3 was found to be 95 nm. From X-ray diffraction intensity versus 2θ, it is explored that the XRD pattern of pristine PPy indicates no sharp peak except a broad peak at $2\theta = 22°–28°$ (Fig. 1a) which is typical peak of PPy and suggests that the nature of PPy is amorphous has been reported [22]. The XRD pattern for PPy-DBSA also amorphous exposed in the range of 20°–30° in Fig. 1b. As in the XRD pattern of PPy-DBSA-Y_2O_3 composite (Fig. 1c) was shifted towards higher angle due
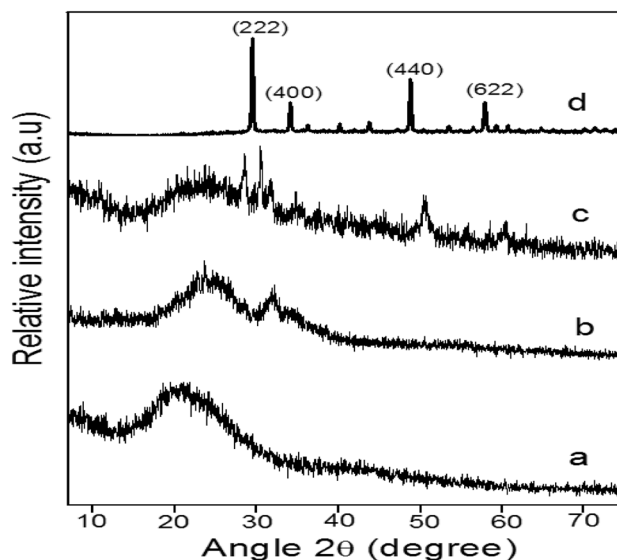

Fig. 1 XRD pattern of (a) PPy, (b) PPy-DBSA, (c) PPy-DBSA-Y_2O_3 (d) pure Y_2O_3

to the intercalation of PPy and Y_2O_3 nanoparticles during the process of synthesis. Consequently, d-values are calculated experimentally via employing Bragg's relation [23]. In Fig. 1c three sharp crystalline peaks of PPy-DBSA-Y_2O_3 at $2\theta = 30.42$, 50.68 and 60.64° resembles with value of $d = 0.15$, 0.99 and 0.088 nm are reduce in composite due to the presence of Y_2O_3 was also observed. Hence, these sharp peaks are openly exhibiting that after mixing Y_2O_3 into the PPy-DBSA crystallinity is enhanced [24].
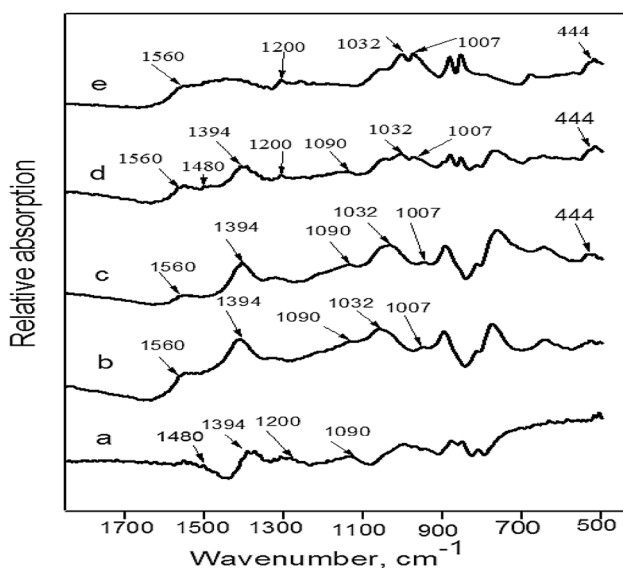

Fig. 2 FTIR spectra of (a) pure PPy (b) PPy-DBSA (c) 2% Y_2O_3 (d) 4% Y_2O_3 and (e) 8% of Y_2O_3 in PPy-DBSA

3.2 FTIR Spectra

FTIR spectra in absorption mode of pure polypyrrole (PPy), PPy-DBSA and composites of PPy-DBSA-Y_2O_3 are publicized in Fig. 2 (curve a–e). The FTIR spectra of PPy and PPy-DBSA (Fig. 2a–b) peak at 1090 cm^{-1} relates to symmetric C–H in the plane mode. The peak at 1200 cm^{-1} is N–H in the plane mode and it was typical absorption peak for PPy. The stretching modes of PPy are established in the region 1600–1400 cm^{-1}. The peak at 1550 cm^{-1} can be assigned for C–C stretching mode of PPy chains [25]. The C=C stretching vibrations at 1560 and 1480 cm^{-1}, C–N and C–C vibrations at 1394 cm^{-1} and C–H out of plane twisted vibration of PPy of polymer chain [26, 27]. Two other peaks of SO_3 near 1032 and 1007 cm^{-1} are identified in doped PPy which are characteristic peaks of sulphonic group [28, 29]. Figure 2c–e demonstrates the FTIR spectra of PPy-DBSA-Y_2O_3 composites which show absorption peaks at 1554 and 1460 cm^{-1} are the individual pyrrole ring vibration furthermore, the peak of metal oxide was observed at 444 cm^{-1}. Thus, these shifts in the peaks in the PPy-DBSA-Y_2O_3 samples show that interfacial interaction exists between the two components.

3.3 Scanning Electron Microscopy

The surface morphology of the samples was investigated by means of Scanning electron microscopy analysis. The SEM micrograph of pure Y_2O_3 nanoparticles and PPy-DBSA-Y_2O_3 composite can be attained and are shown in Fig. 3a and b. In order to substantiate the crystallinity of conducting polypyrrole (PPy) doped with dodecylbenzene sulfonic acid (DBSA) along with yttrium oxide (Y_2O_3)
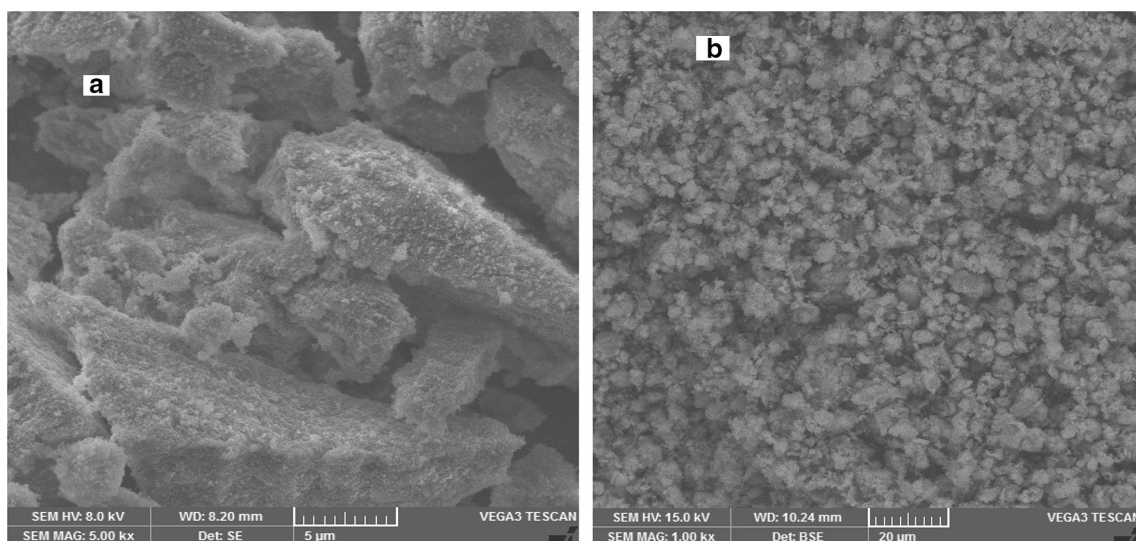

Fig. 3 SEM images of **a** Pure Y_2O_3 and **b** PPy-DBSA-8% Y_2O_3 composite

nanoparticles. Micrograph of pristine polypyrrole show bright granular agglomerates and platelet structure of pure yttrium oxide, however, the particle size of doped polypyrrole enhanced moreover the structure is flakier. From this, it may be concluded that the composite of PPy-DBSA-Y_2O_3 is exhibiting enlargement in particle size moreover a dual structure of platelet in addition to flakier.

3.4 Frequency Dependence of Dielectric Behavior

3.4.1 Dielectric Constant (ε')

The variation of ε' versus frequency (20 Hz to 1 MHz) for PPy, PPy-DBSA along with PPy-DBSA-Y_2O_3 composites with different weight percentage of Y_2O_3 (2%, 4% and 8%) at room temperature is plotted in Fig. 4. The ε' for all samples varies nonlinearly as function of frequency up to 1 MHz. A decrease in ε' was observed by increasing the frequency and it is nearly constant at higher frequencies. At low frequency region dielectric distribution is observed but it becomes nearly independent at high frequency region. Further, we have observed that the values of ε' for these composites are reduces by increasing the weight percentage of Y_2O_3. This can be attributed that the dipoles moving smaller distance within the polymeric chains in the direction of applied field. Conversely, a high value of ε' was observed experimentally at low frequency region due to polarization as well as hopping of charge carriers (polarons and bipolarons) between the localized sites in the system.
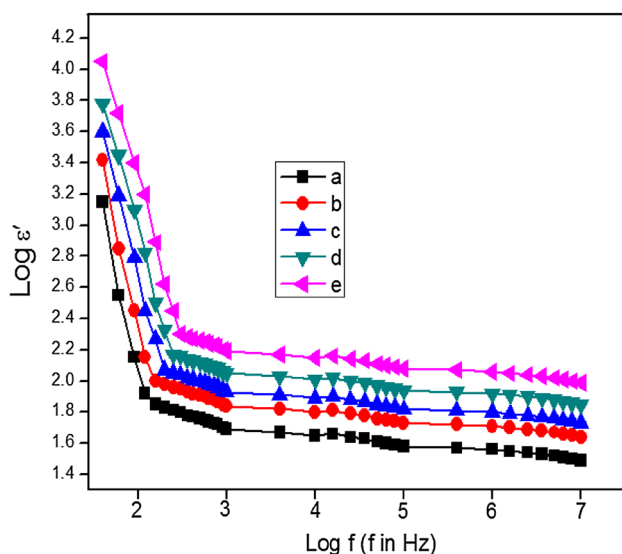
3.4.2 Dielectric Loss (ε'')

The variation of ε'' versus frequency (20 Hz to 1 MHz) for PPy, PPy-DBSA and PPy-DBSA-Y_2O_3 composites with increasing weight percentage of Y_2O_3 at room temperature is exposed in Fig. 5. The ε'' for all samples reduces at low frequency region but it remains constant at higher frequencies. The ε'' was found to be decreases by increasing the frequency as well as it shows that the amount of energy disintegrates in dielectric with applied field. At low frequency region, the presence of insulating grain boundaries and large value of resistivity so required more energy for the hopping of charge carriers between the localized sites. Hence, we observed low value of ε'' at high frequency region because conducting grains present minimum resistance by increasing the weight percentage of Y_2O_3.

3.5 Frequency Dependence of AC Conductivity

The variation in AC conductivity (σ_{ac}) versus frequency ranging from 20 Hz to 1 MHz for PPy, PPy-DBSA and PPy-DBSA-Y_2O_3 composites at room temperature is presented in Fig. 6. Pristine PPy and all the composites show frequency independent AC conductivity at low frequency region and followed high frequency dispersive region where AC conductivity depends upon the frequency and follow a fractional power law. This universal behavior was observed in a present study of synthesized PPy-DBSA-Y_2O_3 composites. The real part of the electrical conductivity $\sigma(\omega)$ can be expressed as:
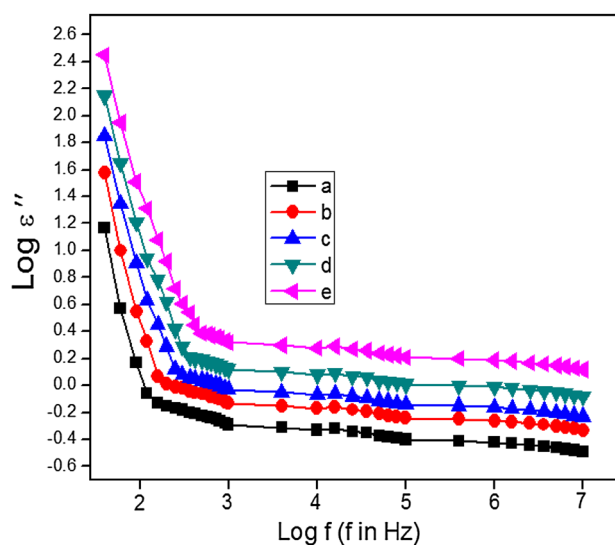
$$\sigma(\omega) = \sigma_0 + A\omega^n \tag{1}$$

Fig. 4 Variation of dielectric constant vs frequency for (a) PPy (b) PPy-DBSA (c) 2% Y_2O_3, (d) 4% Y_2O_3, (e) 8% of Y_2O_3 in PPy-DBSA

Fig. 5 Variation of dielectric loss vs frequency for (a) PPy (b) PPy-DBSA (c) 2% Y_2O_3, (d) 4% Y_2O_3, (e) 8% of Y_2O_3 in PPy-DBSA
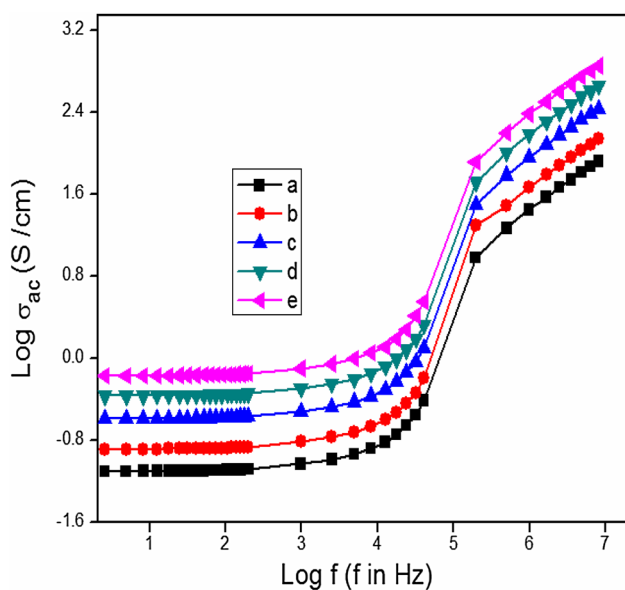
Fig. 6 Variation of AC conductivity vs frequency for (a) PPy, (b) PPy-DBSA (c) 2% Y_2O_3 (d) 4% Y_2O_3 (e) 8% of Y_2O_3 in PPy-DBSA

where σ_0 stands for dc conductivity, "A" pre-exponential factor with units of electrical conductivity, "ω" angular frequency of applied field and "n" is fractional exponent a dimensionless factor. DC conductivity becomes independent of frequency as n approaches to zero, when $n \leq 1$, electrical conductivity depends on frequency [30]. Frequency dependent fractional power law of AC conductivity has been explored variety of disordered materials, for example polymers, amorphous semiconductors along with conducting glasses [31]. Fractional power law (Eq. 1) was employing to observe the hopping of charge carriers (polarons and bipolarons) and also illustrate the AC conduction in conducting polymers [32–34]. AC conductivity enhances as frequency of applied field enhances in disorder polymers due to the hopping of charge carriers (polarons and bipolarons) moving small distance within the polymer chain. From Fig. 6, it is clear that σ_{ac} (ω) increases with increase in frequency which can be due to restricted charges in high frequency region. Thus, fractional power law of AC conductivity was valuable tool to describe the hopping of charge carriers in conducting polymers [35].

4 Conclusions

The different weight percentage of Y_2O_3 nanoparticles based composites of PPy doped DBSA were successfully prepared by in situ polymerization technique. XRD and FTIR results exhibit the intercalation of conducting PPy-DBSA between nano-Y_2O_3 layers and thus, confirm the formation of PPy-DBSA-Y_2O_3 composites. The SEM also confirms the formation of dual phase of platelet as well as flakier structure in PPy-DBSA-Y_2O_3. AC conductivity (σ_{ac}), dielectric constant (ϵ') and loss factor (ϵ'') were enhanced with increased in Y_2O_3 content in PPy-DBSA composites may be suitable candidates for electronic devices applications.

References

1. L.H. Sperling, *Introduction to Physical Polymer Science* (Wiley, Hoboken, 2005)
2. T.Z. Rizvi, A. Shakoor, Electrical conductivity and dielectric properties of polypyrrole/Na + –montmorillonite (PPy/Na + – MMT) clay nanocomposites. J. Phys. D **42**(9), 095415 (2009)
3. R.B. Kaner, A.G. MacDiarmid, Plastics that conduct electricity. Sci. Am. **258**(2), 106–111 (1988)
4. M. Alexandre, P. Dubois, Polymer-layered silicate nanocomposites: preparation, properties and uses of a new class of materials. Mater. Sci. Eng. R **28**(1–2), 1–63 (2000)
5. J. Li, L. Zhu, Y. Wu, Y. Harima, A. Zhang, H. Tang, Hybrid composites of conductive polyaniline and nanocrystalline titanium oxide prepared via self-assembling and graft polymerization. Polymer **47**(21), 7361–7367 (2006)
6. I.H. Campbell, D.L. Smith, Physics of organic electronic devices. Solid State Phys. **55**, 1–117 (2001)
7. M.S. Whittingham, Chemistry of intercalation compounds: metal guests in chalcogenide hosts. Prog. Solid State Chem. **12**(1), 41–99 (1978)
8. R. Clement, M.L. Green, Organometallic intercalates of some lamellar metal phosphorus trisulphides. J. Chem. Soc. Dalton Trans. **10**, 1566–1568 (1979)
9. T.K. Vıshnuvardhan, V.R. Kulkarnı, C. Basavaraja, S.C. Raghavendra, Synthesis, characterization and AC conductivity of polypyrrole/Y_2O_3 composites. Bull. Mater. Sci. **29**(1), 77–83 (2006)
10. Q. Cheng, V. Pavlinek, C. Li, A. Lengalova, Y. He, P. Saha, Synthesis and structural properties of polypyrrole/nano-Y_2O_3 conducting composite. Appl. Surf. Sci. **253**(4), 1736–1740 (2006)
11. J.M. Frechet, D.A. Tomalia, *Dendrimers and Other Dendritic Polymers, Wiley Series in Polymer Science* (Wiley, Hoboken, 2001)
12. M. Thirumal, D. Khastgir, N.K. Singha, B.S. Manjunath, Y.P. Naik, Effect of a nanoclay on the mechanical, thermal and flame retardant properties of rigid polyurethane foam. J. Macromol. Sci. Part A **46**(7), 704–712 (2009)
13. A. Kassim, H.E. Mahmud, F. Adzmi, Polypyrrole–montmorillonite clay composites: an organic semiconductor. Mater. Sci. Semicond. Process. **10**(6), 246–251 (2007)
14. Q. Sun, F.J. Schork, Y. Deng, Water-based polymer/clay nanocomposite suspension for improving water and moisture barrier in coating. Compos. Sci. Technol. **67**(9), 1823–1829 (2007)
15. A. Olad, A. Rashidzadeh, Preparation and anticorrosive properties of PANI/Na-MMT and PANI/O-MMT nanocomposites. Prog. Org. Coat. **62**(3), 293–298 (2008)
16. M. Mravčáková, M. Omastová, P. Pötschke, A. Pozsgay, B. Pukánszky, J. Pionteck, Poly(propylene)/montmorillonite/polypyrrole

composites: structure and conductivity. Polym. Adv. Technol. **17**(9–10), 715–726 (2006)

17. W.S. Huang, B.D. Humphrey, A.G. MacDiarmid, POLYANI-LINE, A. N. C. P., Morphology and chemistry of its oxidation and reduction in aqueous electrolytes. J. Chem. Soc., Faraday Trans. **1**(82), 2385 (1986)

18. R.F. Bianchi, M.F. Panssiera, J.P.H. Lima, L. Yagura, A.M.D. Andrade, R.M. Faria, Spin coater based on brushless dc motor of hard disk drivers. Prog. Org. Coat. **57**(1), 33–36 (2006)

19. G. Gustafsson, G.M. Treacy, Y. Cao, F. Klavetter, N. Colaneri, A.J. Heeger, The, "plastic" led: a flexible light-emitting device using a polyaniline transparent electrode. Synth. Met. **57**(1), 4123–4127 (1993)

20. R.K. Choubey, D. Desai, S.N. Kale, S. Kumar, Effect of annealing treatment and deposition temperature on CdS thin films for CIGS solar cells applications. J. Mater. Sci. **27**(8), 7890–7898 (2016)

21. A.L. Patterson, The Scherrer formula for X-ray particle size determination. Phys. Rev. **56**(10), 978 (1939)

22. Khan, A. S. Preparation, characterization and studies of conducting polymer composites and blends (Doctoral dissertation, Quaid-i-Azam University Islamabad, Pakistan) (2009)

23. W.L. Bragg, The diffraction of short electromagnetic waves by a crystal. Scientia **23**(45), 153 (1929)

24. S. Abdul, Z.R. Tasneem, U.F. Hafiz, H. Najmul, M. Abdul, S. Muhammad, A comparative study of structural, thermal and electrical properties of undoped and doped with dodecylbenzenesulphonic acid polypyrrole. Высокомолекулярные соединения. Серия Б **53**(10), 1833–1838 (2011)

25. S. Saravanan, C.J. Mathai, M.R. Anantharaman, S. Venkatachalam, P.V. Prabhakaran, Investigations on the electrical and structural properties of polyaniline doped with camphor sulphonic acid. J. Phys. Chem. Solids **67**(7), 1496–1501 (2006)

26. B.R. Manjunath, A. Venkataraman, T. Stephen, The effect of moisture present in polymers on their X-ray diffraction patterns. J. Appl. Polym. Sci. **17**(4), 1091–1099 (1973)

27. N. Arsalani, K.E. Geckeler, Novel electrically conducting polymer hybrids with polypyrrole. React. Funct. Polym. **33**(2–3), 167–172 (1997)

28. K.S. Jang, H. Lee, B. Moon, Synthesis and characterization of water soluble polypyrrole doped with functional dopants. Synth. Met. **143**(3), 289–294 (2004)

29. S. Lamprakopoulos, D. Yfantis, A. Yfantis, D. Schmeisser, J. Anastassopoulou, T. Theophanides, An FTIR study of the role of H_2O and D_2O in the aging mechanism of conductive polypyrroles. Synth. Met. **144**(3), 229–234 (2004)

30. S. Yoshimoto, F. Ohashi, T. Kameyama, Simple preparation of sulfate anion-doped polyaniline-clay nanocomposites by an environmentally friendly mechanochemical synthesis route. Macromol. Rapid Commun. **25**(19), 1687–1691 (2004)

31. A.K. Jonscher, *Chelsea Dielectric Press* (Google Scholar, London, 1983)

32. R. Singh, A.K. Narula, R.P. Tandon, A. Mansingh, S. Chandra, Low frequency alternating current conduction and dielectric relaxation in polypyrrole, poly(N-methyl pyrrole), and their copolymers. J. Appl. Phys. **80**(2), 985–992 (1996)

33. P. Dutta, S. Biswas, S.K. De, Alternating-current conductivity and dielectric permittivity of polyaniline doped with β-naphthalene sulphonic acid. J. Phys. **13**(41), 9187 (2001)

34. K.M. Jäger, D.H. McQueen, I.A. Tchmutin, N.G. Ryvkina, M. Klüppel, Electron transport and ac electrical properties of carbon black polymer composites. J. Phys. D **34**(17), 2699 (2001)

35. A.K. Jonscher, The 'universal' dielectric response. Nature **267**(5613), 673 (1977)